UC Davis
UC Davis Previously Published Works

Title

T Cell—Independent Mechanisms Associated with Neutrophil Extracellular Trap Formation and Selective Autophagy in IL-17A—Mediated Epidermal Hyperplasia

Authors

Suzuki, Erika
Maverakis, Emanual
Sarin, Ritu
et al.

T-cell independent mechanisms associated with NETosis and selective autophagy in IL-17A-mediated epidermal hyperplasia

Erika Suzuki[a], **Emanual Maverakis**[c], **Ritu Sarin**[a,b], **Laura Bouchareychas**[a,b], **Vijay K. Kuchroo**[d], **Frank O. Nestle**[e], and **Iannis E. Adamopoulos**[a,f]

[a]Department of Internal Medicine, Division of Rheumatology, Allergy and Clinical Immunology, University of California at Davis, CA, 95616, USA

[c]Department of Dermatology, University of California at Davis, CA, 95616, USA

[d]Center for Neurologic Diseases, Brigham and Women's Hospital, Harvard Medical School, Boston, MA 02115, USA

[e]St. John's Institute of Dermatology, Division of Genetics and Molecular Medicine, King's College London School of Medicine, Guy's Hospital, London, United Kingdom

[f]Institute for Pediatric Regenerative Medicine, Shriners Hospitals for Children Northern California, CA, 95817, USA

Abstract

Interleukin 17A (IL-17A) has been strongly associated with epidermal hyperplasia in many cutaneous disorders. However, as IL-17A is mainly produced by $\alpha\beta$ and $\gamma\delta T$ cells in response to IL-23, the role of T cells and IL-23 have overshadowed any IL-17A independent actions. Herein, we report that IL-17A gene transfer induces epidermal hyperplasia in $Il23r^{-/-}Rag1^{-/-}$ and $Tcr\delta$ deficient mice, which can be prevented by neutrophil depletion. Moreover adoptive transfer of CD11b⁺Gr-1^hi cells, following IL-17A gene transfer, was sufficient to phenocopy the disease. We further show that the IL-17A-induced pathology was prevented in transgenic mice with impaired NETosis and/or neutrophils with conditional deletion of the master regulator of selective autophagy, *Wdfy3*. Our data demonstrate a novel T-cell independent mechanism that is associated with NETosis and selective autophagy in IL-17A-mediated epidermal hyperplasia.

INTRODUCTION

IL-23 and IL-17A have been implicated with epidermal hyperplasia. Although IL-23 partly regulates the expansion of IL-17A producing conventional and non-conventional T cells (Th17 and $\gamma\delta T$ cells respectively), IL-23 can induce epidermal hyperplasia independently of IL-17A via TNF and IL-20R2 dependent mechanisms [1]. Interestingly the IL-23/17 axis does not only regulate T cell differentiation but also neutrophil homeostasis and migration [2],[3]. In agreement with these observations we have also found that gene transfer of either

IL-23 and IL-17 which is associated with epidermal hyperplasia also expands neutrophil populations *in vivo* [4],[5]. In keeping with a role of neutrophils in epidermal hyperplasia others have shown that topical application of a Toll-receptor agonist, imiquimod (IMQ), which stimulates neutrophil function also provokes epidermal hyperplasia in mice [6],[7]. Others demonstrated that in the absence of IL-17RA signaling, IMQ-mediated psoriatic-like skin inflammation is partially reduced indicating that strong association between activation of neutrophils via IL-17 and IMQ and skin inflammation [8].

Although the contribution of Th17 and γδT cells in epidermal hyperplasia is well documented [9],[10],[11],[12], the contribution of activated neutrophils in the observed pathologies is largely unexplored. In order to investigate the role of activated neutrophils in epidermal hyperplasia we performed IL-17 gene transfer to induce neutrophilia and activated neutrophils with IMQ in transgenic mice deficient of Th17 or γδT cells. Our studies uncover T-cell independent mechanisms and a direct role of neutrophils in disease initiation and progression.

A direct role for neutrophils in epidermal hyperplasia is supported by the distinct presence of neutrophil exudates (Munro's microabscesses) in the stratum corneum of the epidermis in psoriasis patients [13],[14]. This is also accompanied by an elevated expression of neutrophil biomarkers associated with neutrophil migration including CXCL1, CXCL8, leukotriene B4 (LTB4) and their receptors, CXCR2 and LTB4R1, and neutrophil derived enzymes including myeloperoxidase (MPO), serpin peptidase inhibitor clade B member 1 (SERPINB1) and Cathepsin G and neutrophil elastase in psoriasis patients [15],[16],[17],[18]. Lysosomal proteins, neutrophil elastase, MPO and SERPINB1, support degradation and elimination of neutrophil phagocytic content through autophagy, a process that requires the assembly of an autophagosome regulated by Wdfy3, the master regulator of macroselective autophagy [19],[20]. Wdfy3 contains a BEACH domain, originally named after the Chediak-Higashi syndrome, a disorder in humans that leads to neutropenia and defects in lysosomal trafficking, resulting in immunodeficiency [21],[20]. In keeping with the putative role of Wdfy3 in neutrophil lysosomal trafficking and inflammation, a recent report demonstrated the requirement of autophagic pathways in NETosis [22], a critical function of neutrophils associated with epidermal hyperplasia and with the secretion of IL-17A [23].

Since neutrophil elastase acts within phagolysosomes to digest phagocytized products, and Wdfy3 is required for the recognition and targeting of the various autophagic cargo for degradation, we primarily tested the hypothesis that NETosis and selective autophagy are critical for epidermal hyperplasia. We validated our observations using neutrophil elastase deficient mice, that are defective in NE, a requirement for NETosis [24] and conditional Wdfy3 deficient mice that are required for selective autophagy. We further confirmed our *in vivo* observations with phorbol 12-myristate 13-acetate (PMA) *in vitro* studies using purified neutrophils that activate NADPH (NOX2)-mediated reactive oxygen species (ROS) production, required for both autophagy and NETosis [22],[25],[26].

Collectively, our data demonstrate that NETosis and selective autophagy may play a role in IL-17A-mediated epidermal hyperplasia and constitute a possible new mechanism, which is independent of IL-23R$^+$ αβ and γδ T cells.

MATERIALS AND METHODS

Reagents and mice

C57BL/6, *Elane$^{-/-}$(NE)$^{-/-}$, Tcrδ$^{-/-}$* and LysM-Cre mice were purchased from Jackson Laboratories (Sacramento, CA). IL-23R^{GFP} reporter mice crossed on RAG1 background and the Wdfy3 floxed mice were previously described [27],[28],[29]. All mice were used between 8–12 wks of age. The University of California at Davis Institutional Animal Care and Use Committee approved all animal protocols. Aldara cream (5% imiquimod) was obtained from 3M Pharmaceuticals. GFP and mouse IL-17A minicircle DNA constructs were produced as previously described [4]. Serum IL-17A was assessed using an ELISA purchased from ebioscience (San Diego, CA). The CXCL1 ELISA kit was purchased from Sigma (St. Louis, MO). The caspase-3 assay was purchased from BioVision. For the neutrophil elastase assay, CD11b$^+$Gr-1^{hi} or Ly6G$^+$ sorted cells were assessed for the presence of NET-associated elastase according to the manufacturer's instructions (Cayman Chemical; Ann Arbor, Michigan). In brief, PMA (20, 50 nM) was used to activate cells for NETosis for 1–4 hrs. DMSO was used as a control for the PMA, washing away unbound neutrophil elastase, followed by a digest of NET DNA by S7 nuclease. The supernatant is taken and later combined with an elastase substrate and the absorbance is read at 405 nm. ROS was assessed using DHR123 (Life Technologies) before analyzed by a microplate reader. Cells were incubated with DPI (NADPH ox. inhibitor) for 1 hr (20 mM) before activating the cells for NETosis. All protocols were followed per manufacturer's instructions.

Western blotting

CD11b$^+$Gr-1^{hi} cells were sorted from the bone marrow of 8 mice per group: WT, LysM^{Cre} and Wdfy3-LysM^{Cre}. The transferred blots were blocked with phospho blocking buffer (Millipore) for 1 hr at room temperature. The antibodies used were: Wdfy3 at 1:1000 (Novus); β-actin at 1:1000 (Cell Signaling); and anti-rabbit IgG HRP at 1:1000 (Cell Signaling). Immunoreactive bands were analyzed by LiCOR using appropriate secondary antibodies.

IL-17A-induced skin inflammation with imiquimod (IMQ)

Eight micrograms of IL-17A of GFP control MC DNA were injected hydrodynamically via retro-orbital delivery. Two days following GFP or IL-17A gene transfer, mouse dorsal fur was shaved and treated with Veet hair removal cream and 20 mg of IMQ was applied to the mouse dorsal skin and assessed the following day. *In vivo* and *ex vivo* imaging was performed using a Maestro 2 *Cri* imager.

Histology

Mouse skins were fixed in 10% formalin buffered in PBS and paraffin embedded for sectioning (6 μm). Tissue sections were stained with hematoxylin and eosin Y (Sigma; St.

Louis, MO). Tissue sections were assessed using a Fluoview FV1000 Confocal Microscope. A licensed dermatologist that was blinded to the experimental conditions assessed epidermal thickening. Epidermal thickness (μm) was determined by measuring the interfollicular epidermal area including or excluding parakeratotic areas and corresponding length on H&E-stained longitudinal paraffin sections from mouse dorsal skin. Analysis and quantification were performed on the Olympus software and in Photoshop CS3 (Adobe).

Cell isolation and flow cytometry

Mice were sacrificed and bone marrow extracts, spleens and skins were collected. Spleens were injected with collagenase D (Sigma) in media (αMEM + 5% FBS + P/S). Total skin was minced using scissors and incubated with digestion buffer (media + 1 U/ml dispase) for 2 hrs at 37°C, followed by addition of collagenase D for 30 min. Digestion was stopped by adding 10 mM EDTA. All tissues were passed through 70-μm cell strainers (BD). Cells were treated with ammonium chloride buffer (150 mM NH_4Cl, 10 mM $KHCO_3$, and 100 μM EDTA) to lyse erythrocytes. Cells were pretreated with anti-CD16/32 mAb for 10 min (to block non-specific binding (BD Biosciences). The cells were stained with anti-CD45 (30-F11, APC), anti-CD11b (M1/70, PB), Annexin V (APC), 7-AAD, anti-Gr-1 (RB6-8C5, PeCy7), anti-Ly6G (1A8, FITC, APC or Pacific Blue; 1A8), anti-CXCR2 (TG11/CXCR2, Alexa 647), and isotype controls were all obtained from Biolegend. Anti-IL-17RA (PAJ-17R, PE) was purchased from ebioscience. AccuCheck counting beads (Life Technologies) were used to determine absolute cell number per cm^2 based on the manufacturer's protocol. Cells were analyzed on a BD FACS ARIA flow cytometer (BD Biosciences). The data were analyzed using FlowJo software (Tree Star, Ashland, OR, USA).

Immunofluorescence

Histology sections (6 μm) of each paraffin block were stained used for immunofluorescence microscopy. Sections were fixed in 4% paraformaldehyde and blocked for 1 hr in blocking buffer (1% triton X, 10% donkey serum in PBS or 2% BSA) then immunostained with DAPI and conjugated antibody against Ly6G (1A8, FITC), neutrophil elastase (Abcam), Wdfy3 (Novus), a donkey anti-goat Alexa 594 secondary and isotype controls (FITC, IgG2a; Alexa Fluor 594 IgG1). CD11b+Gr-1hi or Ly6G+ cells were sorted from the spleen or bone marrow and incubated in RPMI 1640, 1% pen/strep, 1% BSA and allowed to adhere to 0.001% poly-L-lysine coated slides (Thermo Fisher Scientific; Waltham, MA) for 1 hr at 37°C. Neutrophils for neutrophil elastase staining were treated with DMSO or 50 nM PMA for 2 or 4 hrs. The slides were visualized using a confocal microscope (Nikon A1). Fluorescence quantification for neutrophil elastase was performed using ImageJ (National Institutes of Health, Bethesda, MD) to calculate the corrected total cell fluorescence (CTCF = Integrated cell density – (Area of selected cell × Mean fluorescence of background).

Quantification of mRNA levels by real-time PCR

Skin tissue was subject to RNA isolation using the RNeasy kit (Qiagen) including a DNase I digest step. Content and purity of RNA was controlled with a Nanodrop spectrophotometer (Thermo Fisher Scientific). cDNA synthesis was performed using the Omniscript reverse transcription kit (Life Technologies). Quantitative real-time PCR for the candidate genes

was performed using SYBR green chemistry (Agilent) and values were normalized to *Gapdh*. The Ct upper limit was fixed to 40 cycles. Cycling parameters were 95°C (20 s) and 60°C (45 s) in a Mx3005P qPCR machine (Stratagene).

DNA Microarray

Total RNA was isolated from mouse dorsal skins post GFP or IL-17A gene transfer from involved and noninvolved skin at day 3, pooled from 6 mice per group, using a RNasy kit (Qiagen). Biotinylated cDNA was synthesized using the Ovation RNA Amplification System V2 (Nugen) and FL-Ovation cDNA Biotin Module V2 (Nugen), and then hybridized with Mouse Genome 430 2.0 Arrays (Ilumina). Data are deposited in NCBI GEO http://www.ncbi.nlm.nih.gov/geo/query/acc.cgi?acc=GSE86999).

Mouse neutrophil depletion

Neutrophils were depleted using 2 strategies. First, using 500 μg of anti-Ly6G (1A8) antibodies or isotype (IgG2b; LFT-2) as a control two days prior to gene transfer and upon gene transfer. Neutrophil depletion was confirmed on day 2 prior to gene transfer by staining isolated splenocytes with anti-Gr-1 and anti-CD11b antibodies and analyzing the cells by flow cytometry. Secondly, neutrophil depletion was achieved by using cyclophosphamide (CPM) as previously described [30]. PBS injections served as controls for the CPM injections. Neutrophil depletion was confirmed on day 6 prior to gene transfer by staining isolated splenocytes with anti-Gr-1 and anti-CD11b antibodies and analyzing the cells by flow cytometry.

Adoptive transfer of CD11b⁺Gr-1^hi and CD11b⁺Gr-1^lo cells

Splenocytes or bone marrow aspirates from GFP or IL-17A MC-injected mice treated with IMQ on day 3 were sorted for CD11b⁺Gr-1^hi or CD11b⁺Gr-1^lo. Purity of the CD11b⁺Gr-1^hi cells ranged from 90–95%. The cells were labeled with VivoTrack 680 (Perkin Elmer) for 15 min at 37°C, washed 3× with PBS and injected intravenously into naïve recipients (5×10^6 cells per mouse), which were treated the same day with 20 mg of IMQ to shaved dorsal skin. Whole body *in vivo* imaging was performed after 24 hrs using the Maestro 2 *Cri* imager. Optical imaging for VivoTrack 680 was performed using a red filter set (680 nm to 950 nm, long-pass filter). A camera was used to acquire captured images at constant exposure times.

Statistical analysis

Statistical analysis and graphical representations were done using Prism5 software (GraphPad Software). Significant differences in gene expression, imaging, flow cytometry, and epidermal thickening, were assessed using a Mann-Whitney *U*-test or Kruskal-Wallis test followed by post-hoc Dunn's test where appropriate.

ACKNOWLEDGEMENTS

RESULTS

Systemic IL-17A *in vivo* exacerbates epidermal hyperplasia independently of γδT cells and IL-23R

To determine the role of IL-17A *in vivo*, we used a gene transfer approach as previously described with minor modifications [4]. IL-17A was elevated in the serum within 24 hrs and further expanded the CD11b⁺Gr-1ʰⁱ population to be studied (Supplemental Fig. 1A–F). Phenotypic analysis of the expanded CD11b⁺Gr-1ʰⁱ population further confirmed the expression of MPO, as well as CXCR2⁺ and IL-17R⁺, similar to the CD11b⁺Gr-1ʰⁱ cells post GFP gene transfer (Supplemental Fig. 1E–F). Moreover, the expansion of the neutrophils in the periphery post IL-17A gene transfer correlated with an increase in the serum CXCR2 ligand, CXCL1 (Supplemental Fig. 1G). To determine the cellular and molecular mechanisms of epidermal hyperplasia we induced the IL-17A-expanded neutrophil population in mouse dorsal skin with IMQ (a known activator of neutrophils) (Fig. 1A). We performed IMQ dose response and time course experiments post IL-17A gene transfer at low (0, 10, 20 mg) and high (62.5 mg) IMQ concentrations over 5 days to determine a suboptimal dose that could be exacerbated by IL-17A (20 mg) by histology and gene expression analysis (Supplemental Fig. 2A,B). We found that IL-17A gene transfer exacerbated IMQ-induced epidermal hyperplasia in WT mice on day 4 post gene transfer, compared to IMQ-induced GFP MC-injected controls (Fig. 1B,C). Histological analysis of dorsal skin from IL-17A MC-injected mice revealed a mixed cell infiltrate containing neutrophils in the upper epidermis (Munro's microabscesses), along with epidermal hyperplasia (Fig. 1B,C). Immunofluorescence imaging of dorsal skin post IL-17A gene transfer confirmed that neutrophils accumulate in the skin (Fig. 1D; Supplemental Fig. 2C,D,E). Consistent with the histological phenotype, we found an increase in CD11b⁺Gr-1ʰⁱ neutrophils by flow cytometric analysis in the skin (Fig. 1E,F). The increase in CD11b⁺Gr-1ʰⁱ neutrophils correlated with an increase in genes associated with keratinocyte proliferation and skin inflammation including *K16, S100a8, Serpinb1, Cxcl1, Cxcr2* and *Ltb4r1* (Fig. 1G).

To explore whether the effects of IL-17A were independent of IL-23R⁺ T cells and γδT cells, we performed IL-17A gene transfer in *Il23r⁻/⁻Rag1⁻/⁻* and *Tcrδ⁻/⁻* mice. Epidermal hyperplasia was reduced in mice deficient in *Il23r⁻/⁻Rag1⁻/⁻* and *Tcrδ* (Fig. 1H). In keeping with these observations, the IL-17A-associated elevation in CD11b⁺Gr-1ʰⁱ neutrophils in the skin persisted in *Il23r⁻/⁻* and *Tcrδ⁻/⁻* mice (Fig. 1I,J). These data further correlated with an elevation of keratinocyte and inflammatory markers in *Il23r⁻/⁻Rag1⁻/⁻* and *Tcrδ⁻/⁻* mice (Fig. 1K), demonstrating that IL-17A can act independently of IL-23R and T-cell mechanisms to induce skin inflammation.

CD11b⁺Gr-1ʰⁱ cells mediate IL-17A-induced epidermal hyperplasia

To demonstrate whether the CD11b⁺Gr-1ʰⁱ cell population was responsible for inducing epidermal hyperplasia, we performed a neutrophil depletion (Supplemental Fig. 3). Anti-Ly6G significantly reduced the expansion of CD11b⁺Gr-1ʰⁱ cells in the spleen, and skin post IL-17A gene transfer compared to isotype and vehicle controls (Supplemental Fig. 3A–E). The reduction of neutrophils corresponded with a reduction in epidermal thickening,

epidermal hyperplasia, reduced mixed cell infiltrates and a lack of Munro's microabscesses (Fig. 2A,B). Moreover, the reduction in neutrophils was associated with a significantly diminished induction of *K16, S100a8, Serpinb1, Cxcl1, Cxcr2* and *Ltb4r1* in the skin upon IL-17A gene transfer (Fig. 2C). These data indicate that neutrophil depletion suppresses IL-17A-mediated epidermal hyperplasia *in vivo*.

We next performed an adoptive transfer of CD11b⁺Gr-1^hi cells into naïve recipients in the presence of IMQ to evaluate the pathogenicity of neutrophils in the absence of systemic IL-17A expression. We found that CD11b⁺Gr-1^hi but not CD11b⁺Gr-1^lo from IL-17A-gene transfer mice localized to the skin post application of IMQ as detected by VivoTrack 680 [31] labeling (Fig. 2D,E). Histological analysis of mouse dorsal skin showed increased epidermal thickening and evidence of epidermal hyperplasia along with Munro's microabscesses (Fig. 2E,F). Moreover, gene expression of *K16, S100a8, Cxcl1 and Ltb4r1* were elevated upon adoptive transfer with IL-17A MC CD11b⁺Gr-1^hi cells compared to the adoptive transfer of IL-17A MC CD11b⁺Gr-1^lo or GFP MC CD11b⁺Gr-1^hi cells (Fig. 2G). Notably, epidermal hyperplasia was not observed in the control experiments involving adoptive transfer of IL-17A MC CD11b⁺Gr-1^lo or GFP MC CD11b⁺Gr-1^hi, in the presence of IMQ.

Neutrophil elastase is critical for IL-17A-mediated epidermal hyperplasia

We next performed *in vitro* studies on isolated neutrophils to determine whether neutrophil function, (phagocytosis, neutrophil activation or NETosis) is critical to confer pathogenicity in our IL-17A gene transfer model. Neutrophils isolated from IL-17A-gene transfer mice treated with IMQ showed no detectable difference in neutrophil phagocytosis (Fig. 3A) or neutrophil activation (Fig. 3B) compared to GFP-gene transfer controls. However, immunofluorescence staining of sorted CD11b⁺Gr-1^hi cells from IL-17A-gene transfer mice treated with IMQ revealed a marked increase in the expression of neutrophil elastase (NE) compared to controls (Fig. 3C), which also correlated with an increase in NE elastase in the presence of PMA (Fig. 3D). These findings were also confirmed *in vivo* by immunofluorescence imaging of dorsal skins post IL-17A gene transfer and IMQ, which revealed increased NE protein expression compared to controls (Fig. 3E,F). To further elucidate the role of NE, we performed IL-17A gene transfer in combination with IMQ in *Elane* deficient mice (herein referred to as NE⁻/⁻ mice) (Fig. 3G). Histological analysis of dorsal skins from IL-17A MC-injected NE⁻/⁻ mice exhibited reduced epidermal thickening and reduced epidermal hyperplasia and Munro's microabscesses compared to WT controls (Fig. 3H,I). The reduction in skin pathology was consistent with a reduction in gene expression of *K16* (Fig. 3J). The expansion of neutrophils in the spleen (Fig. 3K,L) and the migration of neutrophils to the skin post IL-17A gene transfer and IMQ was not inhibited in NE⁻/⁻ mice (Fig. 3M,N). These data demonstrate that NE plays a critical role in the pathogenesis of IL-17A-mediated skin pathology.

Wdfy3 deficient neutrophils show reduced NETosis, NE and ROS activity

As recent evidence has shown that autophagy is critical for NETosis [22], we next sought to investigate whether deletion of the master regulator of selective autophagy, *Wdfy3*, would affect NETosis. Wdfy3 protein and gene expression was found to be elevated in the inflamed

skin (Supplemental Fig. 4A,B,C). *Wdfy3*^flox/flox mice were crossed with LysM^Cre to selectively ablate *Wdfy3* in myeloid cells to generate *Wdfy3*^flox/flox-LysM^Cre/+ mice (herein referred to as Wdfy3-LysM^Cre). The deletion efficiency of the LysM^Cre was confirmed in CD11b^+Gr-1^hi cells and there was no difference in the total cell number of CD11b^+Gr-1^hi, CD11b^+ and CD11c^+ myeloid cells or any impairment in IL-17A mediated neutrophil expansion, circulation and survival as well as neutrophil priming, activation or phagocytosis (Supplemental Fig. 4D,E,F,G,H) and (data not shown). To assess the role of Wdfy3-LysM^Cre sorted neutrophils in NETosis, we stimulated the cells with PMA. *In vitro* immunofluorescence analysis of Wdfy3-LysM^Cre neutrophils showed that a greater proportion of nuclei were distinct demarcated multilobar rings with uniform DNA staining and had a significant reduction of diffuse nuclei undergoing NETosis, which commonly lacks structure and has a heterogeneous pattern consistent with breakdown of the nuclear envelope, chromatin decondensation and intracellular chromatin dispersion (Fig. 4A,B). Wdfy3-LysM^Cre neutrophils also showed a marked reduction in NET elastase (Fig. 4C) and reduced production of reactive oxygen species (ROS) compared to PMA-treated WT or NE^−/−controls (Fig. 4D).

Wdfy3-LysM^Cre mice are protected against IL-17A-mediated epidermal hyperplasia

To confirm the requirement of *Wdfy3* deficient neutrophils in epidermal hyperplasia we performed IL-17A gene transfer in Wdfy3-LysM^Cre mice (Fig. 5A). Histological analysis of dorsal skins from IL-17A MC-injected Wdfy3-LysM^Cre mice at day 4 revealed reduced epidermal thickening and absence of epidermal hyperplasia and Munro's microabscesses in contrast to WT controls (Fig. 5B,C). Consistent with the histology findings we observed a reduction in gene expression of *K16, S100a8, Cxcl1, Cxcr2 and Ltb4r1* in IL-17A MC-injected Wdfy3-LysM^Cre dorsal skins compared to IL-17A MC-injected WT mice (Fig. 5D). Adoptive transfer of sorted CD11b^+Gr-1^hi cells from Wdfy3-LysM^Cre mice into WT mice failed to induce skin pathology (Fig. 5E,F,G), and this was consistent with a reduction in gene expression of *K16, S100a8, Cxcl1 and Ltb4r1* (Fig. 5H). Taken together, these data demonstrate a novel role for Wdfy3 in mediating neutrophil function via NE in skin inflammation.

DISCUSSION

In our IL-17A gene transfer experiments with γδT cells and *Il23r*^−/−*Rag1*^−/− transgenic mice, we clearly demonstrate IL-23R^+ and T-cell independent mechanisms of IL-17A-induced skin pathology. The induction of epidermal hyperplasia was found to be dependent on CD11b^+Gr-1^hi neutrophils as neutrophil depletion was able to prevent skin pathology. Our data are in agreement with similar studies, whereby conditional overexpression of IL-17A in keratinocytes caused severe psoriasis-like skin inflammation in mice that was reduced by neutrophil depletion [32]. Using the same conditional overexpression of IL-17A in keratinocytes other studies have also supported the role of IL-17A in neutrophil associated Munro's microabscesses through IL-6 [33]. This data are also in agreement with our previous findings where gene transfer of IL-17 also elevated serum IL-6 in vivo and was associated with skin inflammation and neutrophil exudates [4]. Although it is agreed that there is prominent formation of neutrophil-rich Munro's microabscesses, (a clinical marker

with the highest histological occurrence for the diagnosis of psoriasis) [34] little is known about the neutrophil cellular and molecular mechanisms that confer pathogenicity.

Recent reports have highlighted novel roles for the function of neutrophils in destructive diseases that are dependent on NETosis, a unique form of cell death that is characterized by the release of decondensed chromatin and granular contents to the extracellular space [35]. Indeed it has been reported that NETosis is prominent in necrotic areas and the prevention of NET release eliminates tissue damage in liver tissue [36]. Specifically, inhibition of NE, an enzyme implicated in the initial decondensation of DNA and the proteolytic degradation of the nuclear envelope, diminished damage to the liver [36]. In keeping with these observations, other groups have also shown that NE is critical in the formation of NETs and mouse peritoneal neutrophils derived from NE deficient mice lack nuclear decondensation activity *in vitro* and fail to form NETs [24]. We also found that neutrophils isolated from IL-17A-gene transfer mice in the presence of IMQ had elevated NE expression and *in vivo* this expression was localized within the inflamed skin. Furthermore, as NE$^{-/-}$ mice were protected from IL-17A-mediated epidermal hyperplasia, our data demonstrate NE to be critical for disease pathogenesis.

In keeping with these observations other reports have also shown that neutrophils isolated from blood of psoriatic patients show frequent NET formation and NET-associated enzymes are further localized in psoriatic lesions [23]. Furthermore it was recently shown that NETosis requires autophagy and the generation of superoxide [22]. To investigate the role of autophagy in this process we blocked the selective macroautophagy pathway by ablating Wdfy3, an adaptor protein responsible for the degradation of aggregated proteins in macroautophagy [19]. Interestingly, Wdfy3, contains a BEACH domain, which has been associated with neutropenia and defects in lysosomal trafficking, in Chediak-Higashi Syndrome [21],[20].

Wdfy3, the master regulator of selective macroautophagy, similarly to NE, was also highly expressed in neutrophils *in vitro*, and *in vivo* this expression was localized within the inflamed skin. Our cre-lox system approach with a LysM promoter to selectively ablate Wdfy3 in myeloid cells also resulted in protection from disease. Although LysM is not specific to neutrophils and is found in various myeloid cells, our adaptive transfer of CD11b$^+$Gr-1^{hi} cells from IL-17A-gene transfer mice and the fact that IL-17A gene transfer did not induce any other myeloid population (data not shown), confirmed the specificity. Moreover, there were no detectable differences in the percent of apoptotic or necrotic neutrophils in the absence of Wdfy3, nor an apparent difference in the priming, activation or phagocytic capacity of the *Wdfy3*-deficient neutrophils compared to controls suggesting that no other neutrophil function was impaired in the *Wdfy3*-deficient neutrophils. We further confirmed our observations using phorbol myristate acetate (PMA)-stimulated neutrophils as previously described by Remijsen et al [22]. Our data showed that *Wdfy3*-deficient neutrophils exhibit a marked reduction in intracellular ROS compared to controls, suggesting that Wdfy3 may attenuate NETosis via modulating ROS.

Although our data identify NETosis as a major player in the pathogenesis of epidermal hyperplasia other cellular mechanisms may also contribute. For instance, on a cellular level,

nucleic acids can induce myeloid cell activation to stimulate the secretion of various pro-inflammatory cytokines to recruit inflammatory cells such as neutrophils, which in the presence of stimulatory cytokines and danger signals promote the cycle of inflammation within the skin [37]. As neutrophil elastase deficiency in mice can lead to increased susceptibility to infections [38], it is possible that *Wdfy3* may be a more suitable target with a higher therapeutic potential.

Collectively, these results identify Wdfy3 as novel regulator of neutrophil function, which may be exploited to debilitate neutrophil function as a therapeutic approach in cutaneous disorders such as psoriasis.

Supplementary Material

Refer to Web version on PubMed Central for supplementary material.

Acknowledgments

REFERENCES

1. Chan JR, Blumenschein W, Murphy E, Diveu C, Wiekowski M, Abbondanzo S, Lucian L, Geissler R, Brodie S, Kimball AB, et al. IL-23 stimulates epidermal hyperplasia via TNF and IL-20R2-dependent mechanisms with implications for psoriasis pathogenesis. The Journal of experimental medicine. 2006; 203(12):2577–2587. [PubMed: 17074928]

2. Lemos HP, Grespan R, Vieira SM, Cunha TM, Verri WA Jr, Fernandes KS, Souto FO, McInnes IB, Ferreira SH, Liew FY, et al. Prostaglandin mediates IL-23/IL-17-induced neutrophil migration in inflammation by inhibiting IL-12 and IFNgamma production. Proc Natl Acad Sci U S A. 2009; 106(14):5954–5959. [PubMed: 19289819]

3. Smith E, Zarbock A, Stark MA, Burcin TL, Bruce AC, Foley P, Ley K. IL-23 is required for neutrophil homeostasis in normal and neutrophilic mice. J Immunol. 2007; 179(12):8274–8279. [PubMed: 18056371]

4. Adamopoulos IE, Suzuki E, Chao CC, Gorman D, Adda S, Maverakis E, Zarbalis K, Geissler R, Asio A, Blumenschein WM, et al. IL-17A gene transfer induces bone loss and epidermal hyperplasia associated with psoriatic arthritis. Ann Rheum Dis. 2015; 74(6):1284–1292. [PubMed: 24567524]

5. Adamopoulos IE, Tessmer M, Chao CC, Adda S, Gorman D, Petro M, Chou CC, Pierce RH, Yao W, Lane NE, et al. IL-23 is critical for induction of arthritis, osteoclast formation, and maintenance of bone mass. J Immunol. 2011; 187(2):951–959. [PubMed: 21670317]

6. van der Fits L, Mourits S, Voerman JS, Kant M, Boon L, Laman JD, Cornelissen F, Mus AM, Florencia E, Prens EP, et al. Imiquimod-induced psoriasis-like skin inflammation in mice is mediated via the IL-23/IL-17 axis. J Immunol. 2009; 182(9):5836–5845. [PubMed: 19380832]

7. Hayashi F, Means TK, Luster AD. Toll-like receptors stimulate human neutrophil function. Blood. 2003; 102(7):2660–2669. [PubMed: 12829592]

8. El Malki K, Karbach SH, Huppert J, Zayoud M, Reissig S, Schuler R, Nikolaev A, Karram K, Munzel T, Kuhlmann CR, et al. An alternative pathway of imiquimod-induced psoriasis-like skin inflammation in the absence of interleukin-17 receptor a signaling. The Journal of investigative dermatology. 2013; 133(2):441–451. [PubMed: 22951726]

9. Cai Y, Shen X, Ding C, Qi C, Li K, Li X, Jala VR, Zhang HG, Wang T, Zheng J, et al. Pivotal role of dermal IL-17-producing gammadelta T cells in skin inflammation. Immunity. 2011; 35(4):596–610. [PubMed: 21982596]

10. Pantelyushin S, Haak S, Ingold B, Kulig P, Heppner FL, Navarini AA, Becher B. Rorgammat+ innate lymphocytes and gammadelta T cells initiate psoriasiform plaque formation in mice. The Journal of clinical investigation. 2012; 122(6):2252–2256. [PubMed: 22546855]

11. Nishimoto S, Kotani H, Tsuruta S, Shimizu N, Ito M, Shichita T, Morita R, Takahashi H, Amagai M, Yoshimura A. Th17 cells carrying TCR recognizing epidermal autoantigen induce psoriasis-like skin inflammation. J Immunol. 2013; 191(6):3065–3072. [PubMed: 23956432]

12. Becher B, Pantelyushin S. Hiding under the skin: Interleukin-17-producing gammadelta T cells go under the skin? Nature medicine. 2012; 18(12):1748–1750.

13. Nestle FO, Kaplan DH, Barker J. Psoriasis. The New England journal of medicine. 2009; 361(5): 496–509. [PubMed: 19641206]

14. Perera GK, Di Meglio P, Nestle FO. Psoriasis. Annual review of pathology. 2012; 7:385–422.

15. Schonthaler HB, Guinea-Viniegra J, Wculek SK, Ruppen I, Ximenez-Embun P, Guio-Carrion A, Navarro R, Hogg N, Ashman K, Wagner EF. S100A8–S100A9 protein complex mediates psoriasis by regulating the expression of complement factor C3. Immunity. 2013; 39(6):1171–1181. [PubMed: 24332034]

16. Kulke R, Bornscheuer E, Schluter C, Bartels J, Rowert J, Sticherling M, Christophers E. The CXC receptor 2 is overexpressed in psoriatic epidermis. The Journal of investigative dermatology. 1998; 110(1):90–94. [PubMed: 9424095]

17. Lessard JC, Pina-Paz S, Rotty JD, Hickerson RP, Kaspar RL, Balmain A, Coulombe PA. Keratin 16 regulates innate immunity in response to epidermal barrier breach. Proceedings of the National Academy of Sciences of the United States of America. 2013; 110(48):19537–19542. [PubMed: 24218583]

18. Henry CM, Sullivan GP, Clancy DM, Afonina IS, Kulms D, Martin SJ. Neutrophil-Derived Proteases Escalate Inflammation through Activation of IL-36 Family Cytokines. Cell reports. 2016; 14(4):708–722. [PubMed: 26776523]

19. Filimonenko M, Isakson P, Finley KD, Anderson M, Jeong H, Melia TJ, Bartlett BJ, Myers KM, Birkeland HC, Lamark T, et al. The selective macroautophagic degradation of aggregated proteins requires the PI3P-binding protein Alfy. Molecular cell. 2010; 38(2):265–279. [PubMed: 20417604]

20. Lekstrom-Himes JA, Gallin JI. Immunodeficiency diseases caused by defects in phagocytes. The New England journal of medicine. 2000; 343(23):1703–1714. [PubMed: 11106721]

21. Jiang S, Dupont N, Castillo EF, Deretic V. Secretory versus degradative autophagy: unconventional secretion of inflammatory mediators. Journal of innate immunity. 2013; 5(5):471–479. [PubMed: 23445716]

22. Remijsen Q, Vanden Berghe T, Wirawan E, Asselbergh B, Parthoens E, De Rycke R, Noppen S, Delforge M, Willems J, Vandenabeele P. Neutrophil extracellular trap cell death requires both autophagy and superoxide generation. Cell research. 2011; 21(2):290–304. [PubMed: 21060338]

23. Lin AM, Rubin CJ, Khandpur R, Wang JY, Riblett M, Yalavarthi S, Villanueva EC, Shah P, Kaplan MJ, Bruce AT. Mast cells and neutrophils release IL-17 through extracellular trap formation in psoriasis. J Immunol. 2011; 187(1):490–500. [PubMed: 21606249]

24. Papayannopoulos V, Metzler KD, Hakkim A, Zychlinsky A. Neutrophil elastase and myeloperoxidase regulate the formation of neutrophil extracellular traps. The Journal of cell biology. 2010; 191(3):677–691. [PubMed: 20974816]

25. Remijsen Q, Kuijpers TW, Wirawan E, Lippens S, Vandenabeele P, Vanden Berghe T. Dying for a cause: NETosis, mechanisms behind an antimicrobial cell death modality. Cell death and differentiation. 2011; 18(4):581–588. [PubMed: 21293492]

26. Brinkmann V, Reichard U, Goosmann C, Fauler B, Uhlemann Y, Weiss DS, Weinrauch Y, Zychlinsky A. Neutrophil extracellular traps kill bacteria. Science. 2004; 303(5663):1532–1535. [PubMed: 15001782]

27. Awasthi A, Riol-Blanco L, Jager A, Korn T, Pot C, Galileos G, Bettelli E, Kuchroo VK, Oukka M. Cutting edge: IL-23 receptor gfp reporter mice reveal distinct populations of IL-17-producing cells. J Immunol. 2009; 182(10):5904–5908. [PubMed: 19414740]

28. Orosco LA, Ross AP, Cates SL, Scott SE, Wu D, Sohn J, Pleasure D, Pleasure SJ, Adamopoulos IE, Zarbalis KS. Loss of Wdfy3 in mice alters cerebral cortical neurogenesis reflecting aspects of the autism pathology. Nature communications. 2014; 5:4692.

29. Wu DJ, Gu R, Sarin R, Zavodovskaya R, Chen CP, Christiansen BA, Adamopoulos IE. Autophagy-linked FYVE containing protein WDFY3 interacts with TRAF6 and modulates RANKL-induced osteoclastogenesis. Journal of autoimmunity. 2016

30. Oyoshi MK, He R, Li Y, Mondal S, Yoon J, Afshar R, Chen M, Lee DM, Luo HR, Luster AD, et al. Leukotriene B4-driven neutrophil recruitment to the skin is essential for allergic skin inflammation. Immunity. 2012; 37(4):747–758. [PubMed: 23063331]

31. Peterson JD, Labranche TP, Vasquez KO, Kossodo S, Melton M, Rader R, Listello JT, Abrams MA, Misko TP. Optical tomographic imaging discriminates between disease-modifying anti-rheumatic drug (DMARD) and non-DMARD efficacy in collagen antibody-induced arthritis. Arthritis research & therapy. 2010; 12(3):R105. [PubMed: 20509880]

32. Karbach S, Croxford AL, Oelze M, Schuler R, Minwegen D, Wegner J, Koukes L, Yogev N, Nikolaev A, Reissig S, et al. Interleukin 17 drives vascular inflammation, endothelial dysfunction, and arterial hypertension in psoriasis-like skin disease. Arteriosclerosis, thrombosis, and vascular biology. 2014; 34(12):2658–2668.

33. Croxford AL, Karbach S, Kurschus FC, Wortge S, Nikolaev A, Yogev N, Klebow S, Schuler R, Reissig S, Piotrowski C, et al. IL-6 regulates neutrophil microabscess formation in IL-17A-driven psoriasiform lesions. The Journal of investigative dermatology. 2014; 134(3):728–735. [PubMed: 24067382]

34. Johnson MA, Armstrong AW. Clinical and histologic diagnostic guidelines for psoriasis: a critical review. Clinical reviews in allergy & immunology. 2013; 44(2):166–172. [PubMed: 22278173]

35. Brinkmann V, Zychlinsky A. Neutrophil extracellular traps: is immunity the second function of chromatin? The Journal of cell biology. 2012; 198(5):773–783. [PubMed: 22945932]

36. Kolaczkowska E, Jenne CN, Surewaard BG, Thanabalasuriar A, Lee WY, Sanz MJ, Mowen K, Opdenakker G, Kubes P. Molecular mechanisms of NET formation and degradation revealed by intravital imaging in the liver vasculature. Nature communications. 2015; 6:6673.

37. Pasparakis M, Haase I, Nestle FO. Mechanisms regulating skin immunity and inflammation. Nature reviews Immunology. 2014; 14(5):289–301.

38. Belaaouaj A, McCarthy R, Baumann M, Gao Z, Ley TJ, Abraham SN, Shapiro SD. Mice lacking neutrophil elastase reveal impaired host defense against gram negative bacterial sepsis. Nature medicine. 1998; 4(5):615–618.
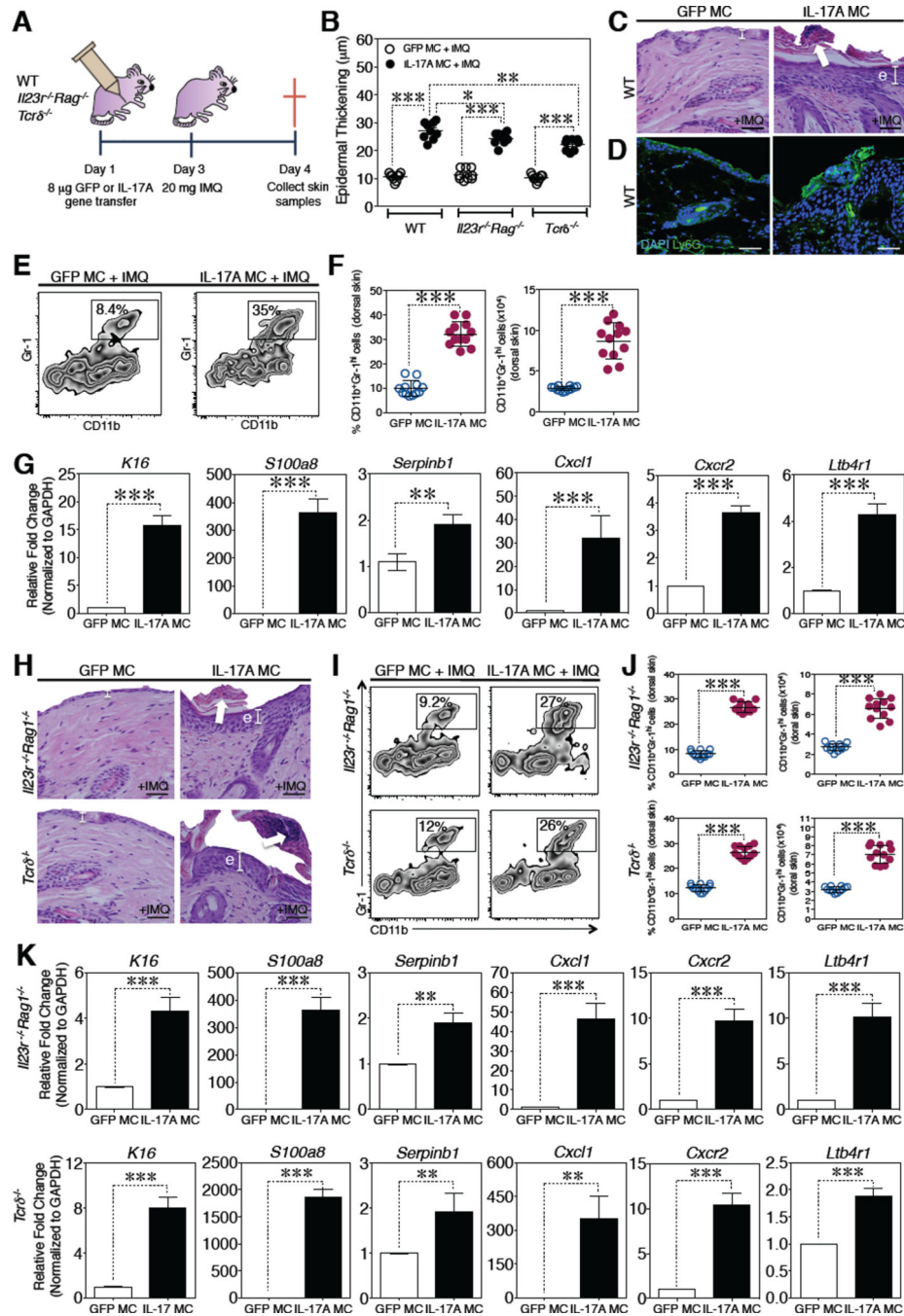
Fig. 1. Systemic IL-17A expression *in vivo* exacerbates imiquimod (IMQ)-induced epidermal hyperplasia independently of IL-23R+ T cells and γδT cells

(**A**) Schematic of GFP or IL-17A gene transfer model with IMQ in WT, *Il23r−/−Rag1−/−* and *Tcrδ−/−* mice at 4 days post GFP or IL-17A gene transfer and IMQ. (**B**) Quantification of epidermal thickening (μm) in WT, *Il23r−/−Rag1−/−* and *Tcrδ−/−* mice, (**C**) histological analysis and (**D**) immunofluorescence images of Ly6G+ cells in WT dorsal skins post gene transfer. Images are representative of 3 independent experiments, 3 mice per group. Bar, 40 μm. Arrow indicates Munro's microabscess, e = epidermal hyperplasia. (**E**) Flow cytometric

analysis of CD11b$^+$Gr-1^{hi} cells gated on CD45$^+$ cells in WT skin (n = 4 per group (GFP or IL-17A MC), 3 independent experiments). (**F**) Plots indicate the percentage of and absolute CD11b$^+$Gr-1^{hi} cell number in the skin. (**G**) Gene expression analysis of *K16, S100a8, Serpinb1, Cxcl1, Cxcr2* and *Ltb4r1* in WT skin (n = 3 per group, 3 independent experiments). (**H**) Histological analysis of *Il23r$^{-/-}$Rag1$^{-/-}$* or *Tcrδ$^{-/-}$* dorsal skins. Images are representative of 3 independent experiments, 3 mice per group. Bar, 20 μm. Arrow indicates Munro's microabscess, e = epidermal hyperplasia. (**I**) Flow cytometric analysis of CD11b$^+$Gr-1^{hi} cells gated on CD45$^+$ cells in *Il23r$^{-/-}$Rag1$^{-/-}$* or *Tcrδ$^{-/-}$* skin (n = 4 per group, 3 independent experiments). (**J**) Plots to the right indicate the percentage and absolute CD11b$^+$Gr-1^{hi} cell number in the skin. (**K**) Gene expression analysis of *K16, S100a8, Serpinb1, Cxcl1, Cxcr2* and *Ltb4r1* in *Il23r$^{-/-}$Rag1$^{-/-}$* or *Tcrδ$^{-/-}$* skin (n = 4 per group, 3 independent experiments). Data represent mean ± SEM. *p<0.05, **p<0.01, ***p<0.001, using a Mann-Whitney *U*-test. Significant differences in (B) were determined using Kruskal-Wallis test followed by post-hoc Dunn's test.
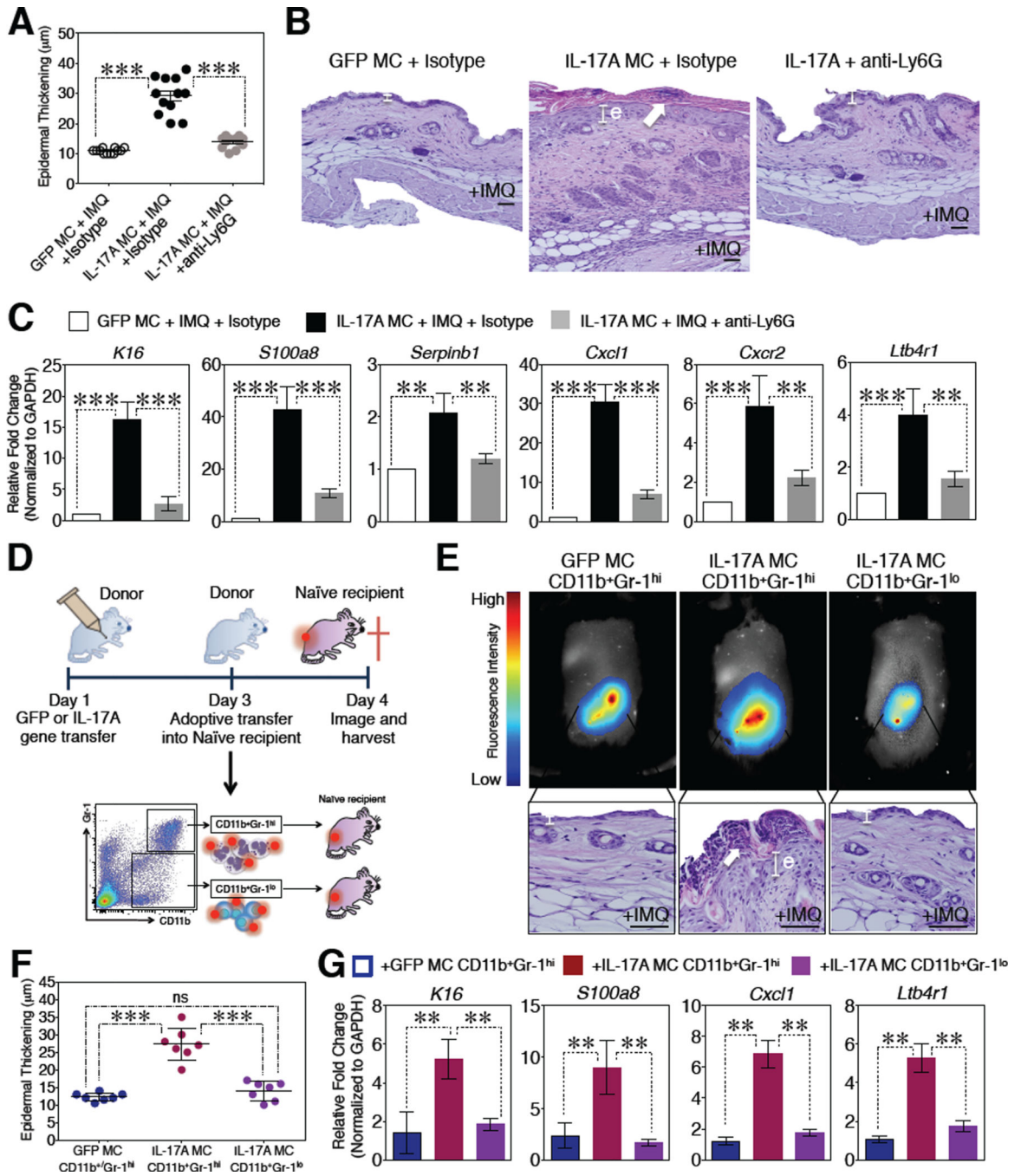
Fig. 2. CD11b+Gr-1hi cells mediate IL-17A-induced epidermal hyperplasia
(**A**) Quantification of epidermal thickening (μm) and (n = 3 per group, 3 independent experiments). (**B**) histological analysis of mouse dorsal skins at day 4 post gene transfer, IMQ and neutrophil depletion with anti-Ly6G. Images are representative of 2 independent experiments, 6 mice per group. Arrow indicates Munro's microabscess, e = epidermal hyperplasia. Bar, 40 μm. (**C**) Gene expression analysis of *K16, S100a8, Serpinb1, Cxcl1, Cxcr2* and *Ltb4r1* in dorsal skin at day 4 post gene transfer, IMQ and anti-Ly6G (n = 6 per group, 2 independent experiments). (**D**) Schematic of adoptive transfer of CD11b+Gr-1lo or

CD11b$^+$Gr-1^{hi} cells sorted at day 3 post GFP or IL-17A gene transfer. Subsequently, cells were labeled with Vivotrack 680 and injected intravenously into naïve mice treated with IMQ. (**E**) Imaging of Vivotrack 680-labeled cells in (D) (*top*) 24 hrs post adoptive transfer. Histological analysis of dorsal skin 24 hrs post adoptive transfer of cells in (D) (*bottom*). Images are representative of 2 independent experiments, 3–4 mice per group. Bar, 40 μm. (**F**) Quantification of epidermal thickening (μm) and (**G**) gene expression of *K16, S100a8, Cxcl1* and *Ltb4r1* in mouse dorsal skins 24 hrs post adoptive transfer of cells in (D). (n = 3–4 per group, 2 independent experiments). Data represent mean ± SEM. *p<0.05, **p<0.01, ***p<0.001, using a Kruskal-Wallis test followed by post-hoc Dunn's test.
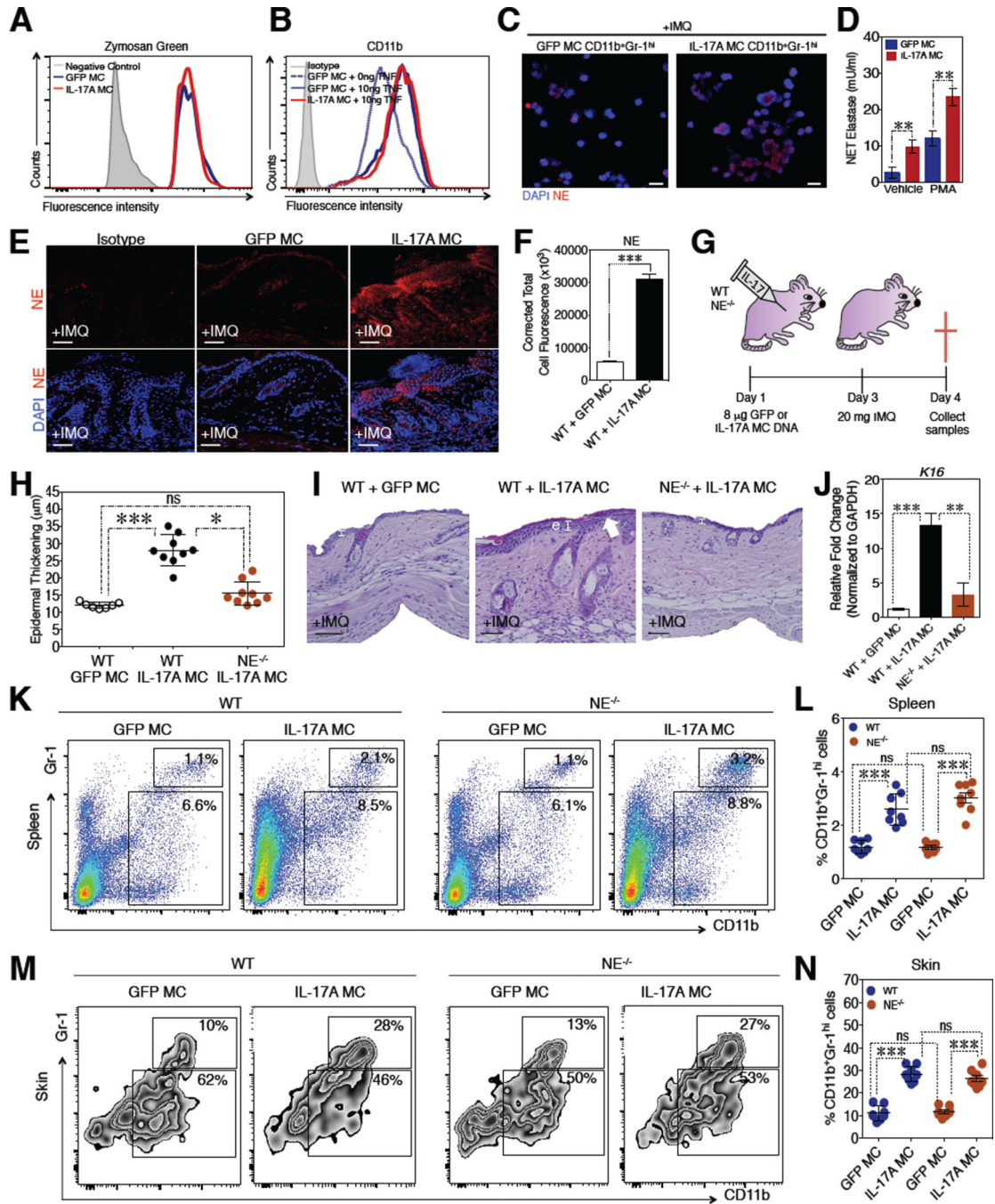
Fig. 3. NE is critical for IL-17A-mediated epidermal hyperplasia

(**A**) Flow cytometric phagocytic analysis of zymosan green beads engulfed by CD11b$^+$Gr-1^{hi} or (**B**) CD11b expression post 30 min treatment with 0 or 10 ng/ml of TNF on FACS-sorted CD11b$^+$Gr-1^{hi} cells isolated from the bone marrow post GFP or IL-17A gene transfer and IMQ (n = 3 per group, 3 independent experiments). (**C**) Immunofluorescence staining of neutrophil elastase or nuclei (DAPI) in cytopsin preparations of sorted CD11b$^+$Gr-1^{hi} cells from bone marrow of GFP or IL-17A-gene transfer mice with IMQ (n = 3 per group, 3 independent experiments). (**D**) Quantitative

analysis of NET-associated elastase in GFP or IL-17A-gene transfer CD11b$^+$Gr-1^{hi} cells treated with vehicle or 50 nM PMA as in (C) (n = 4 per group, 3 independent experiments). Bar, 10 μm. (**E**) Immunofluorescence staining of neutrophil elastase in the skin post gene transfer with IMQ in WT mice and (**F**) quantification of neutrophil elastase staining. (**G**) Schematic of the gene transfer model with IMQ in WT and NE$^{-/-}$ mice. (**H**) Quantification of epidermal thickening (μm), (**I**) histological analysis, (**J**) gene expression analysis of *K16*, and flow cytometric analysis of CD11b$^+$Gr-1^{hi} cells in WT or NE$^{-/-}$ spleen (**K,L**) and dorsal skin (**M,N**) at 4 days post gene transfer and IMQ. Bar, 20 μm. (n = 4 per group, 3 independent experiments). Images are representative of 3 independent experiments, 4 mice per group. Arrow indicates Munro's microabscess, e = epidermal hyperplasia. Data represent mean ± SEM. *p<0.05, **p<0.01, ***p<0.001, using a Kruskal-Wallis test followed by post-hoc Dunn's test.
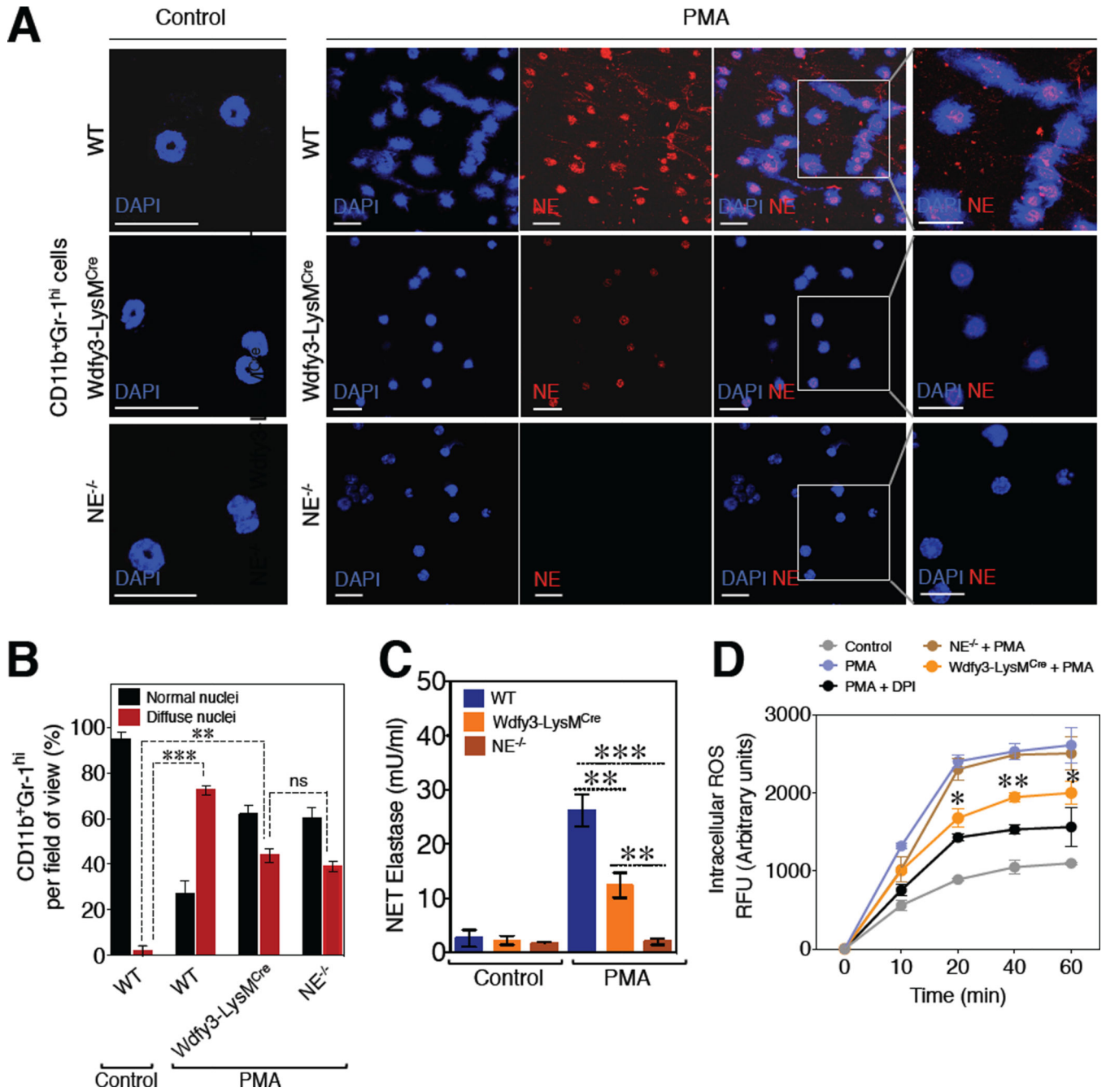
Fig. 4. Wdfy3 deficient neutrophils show reduced NETosis, NE and ROS activity
(**A**) Immunofluorescence staining of neutrophil elastase (NE) or nuclei (DAPI) in sorted CD11b^{+}Gr-1^{hi} cells from bone marrow of naïve WT, Wdfy3-LysM[Cre] or $NE^{-/-}$ mice treated with vehicle (DMSO) or PMA, and (**B**) quantitative analysis of normal and diffuse nuclei in WT, Wdfy3-LysM[Cre] or $NE^{-/-}$ mice (n = 3 per group, 3 independent experiments). Bar, 10 μm. (**C**) Quantitative analysis of NET-associated elastase in naïve CD11b^{+}Gr-1^{hi} cells treated with vehicle or PMA as in (C) (n = 4 per group, 3 independent experiments). Data represent mean ± SEM. **p<0.01, ***p<0.001, using a Kruskal-Wallis test followed by post-hoc Dunn's test. (**D**) Plate reader assay of intracellular reactive oxygen species
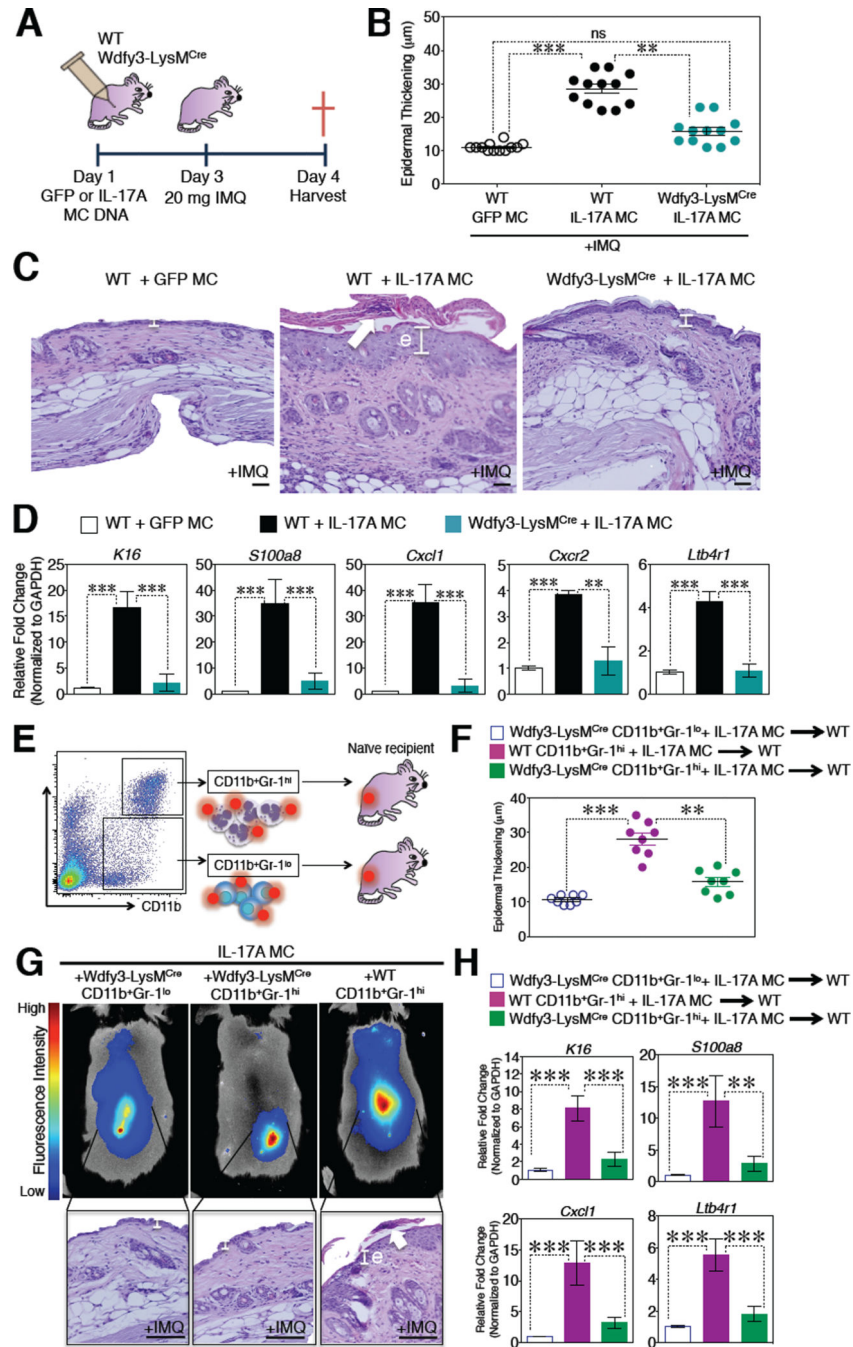
generation in CD11b$^+$Gr-1^{hi} cells isolated from bone marrow of naïve WT, Wdfy3-LysM^{Cre} or $NE^{-/-}$ mice treated with either control (DMSO), PMA or DPI (NADPH ox. inhibitor) using DHR123 (n = 4 per group, 3 independent experiments). Data represent mean ± SEM. and ns = non significant, *p<0.05, **p<0.01, using a two-way ANOVA.

Fig. 5. Wdfy3-LysM^Cre mice are protected against IL-17A-mediated epidermal hyperplasia
(**A**) Schematic of the gene transfer model with IMQ in WT and Wdfy3-LysM^Cre mice. (**B**) Quantification of epidermal thickening (μm), (**C**) histological analysis and (**D**) gene expression analysis of *K16, S100a8, Cxcl1, Cxcr2* and *Ltb4r1* in WT or Wdfy3-LysM^Cre dorsal skin at 4 days post gene transfer and IMQ. (n = 4 per group, 3 independent experiments). Images are representative of 3 independent experiments, 4 mice per group. Arrow indicates Munro's microabscess, e = epidermal hyperplasia. Bar, 20 μm. (**E**) Schematic of CD11b^+Gr-1^hi or CD11b^+Gr-1^lo cells sorted from WT or Wdfy3-LysM^Cre

mice post GFP or IL-17A gene transfer and IMQ and labeled with Vivotrack 680, then intravenously injected into naïve WT mice treated with IMQ. (**F**) Quantification of epidermal thickening (μm) in mice post adoptive transfer of CD11b+Gr-1hi or CD11b+Gr-1lo cells sorted from IL-17A-MC injected WT or Wdfy3-LysMCre mice and IMQ into naïve WT recipient mouse dorsal skins treated with IMQ (n = 4 per group, 2 independent experiments). (**G**) Imaging (*top*) and histological analysis (*bottom*) of CD11b+Gr-1hi or CD11b+Gr-1lo cells isolated from Wdfy3-LysMCre mice, imaged at 24 hrs post adoptive transfer and IMQ application (*top*). Images are representative of 2 independent experiments, 4 mice per group. Bar, 20 μm. (**H**) Gene expression of *K16, S100a8, Cxcl1* and *Ltb4r1* in WT skin 24 hrs post adoptive transfer of CD11b+Gr-1hi or CD11b+Gr-1lo cells from WT or Wdfy3-LysMCre mice treated with IMQ (n = 4 per group, 2 independent experiments). Data represent mean ± SEM. *p<0.05, **p<0.01, ***p<0.001, using a Kruskal-Wallis test followed by post-hoc Dunn's test.